2014 IEEE International Conference on Robotics & Automation (ICRA)
Hong Kong Convention and Exhibition Center
May 31 - June 7, 2014. Hong Kong, China

A Reduced-Gravity Simulator for Physically Simulating Human Walking in Microgravity or Reduced-Gravity Environment

Wenwu Xiu, Kenneth Ruble, and Ou Ma, *Member, IEEE*

***Abstract*— Astronauts must go through extensive training of their tasks in a simulated microgravity or reduced-gravity environment before they can perform the same tasks in space. Scientists and engineers also need simulated reduced-gravity facilities to study human performance and factors in space. This paper presents a novel design and prototype test of a multi-DOF reduced-gravity simulator which can be used for training astronauts and studying human factors in zero or partial gravity environment. Designed based on the passive static balancing technology, the simulator can passively compensate the gravity force applied to a human to any level from 0 to 100% at all the configurations within its workspace. Therefore, a person attached to the simulator can biomechanically feel like he/she were in a real reduced-gravity environment while doing a physical activity such as walking or jumping. A prototype of the simulator was developed to study the feasibility and dynamic performance of the system. The prototype study demonstrated the reduced-gravity simulation capability of the system. It also revealed some interesting findings which motivate further research in the future.**

I. Introduction

In human space exploration missions, astronauts are often required to perform various intra-vehicle activities (IVA) and extra-vehicle activities (EVA) tasks. Such work is done either in a microgravity environment such as in the International Space Station or in a reduced-gravity environment such as on the Moon or Mars. To properly plan and prepare those human tasks, astronauts are required to perform extensive training of these tasks in simulated reduced-gravity (reduced-G) facilities before a real mission can be launched. Astronauts usually spend over ten times the real EVA time in a ground-based microgravity training facility such as a neural buoyancy pool to practice a planned EVA task. Similarly, space operations engineers usually spend much more than the real EVA time to plan and analyze an EVA/IVA task. Therefore, the training technology and facility have a significant impact on the quality and cost of the EVA/IVA planning and training.

Several existing technologies can be used for EVA training in a simulated reduced-G environment, such as the water-based neutral buoyancy [1], parabolic-trajectory flight, counter-weight suspension [2], cable-based suspension [3], air-bearing/gimbal support [4] and virtual reality [5], etc. All of these have some drawbacks when used for physical simulation of reduced-G environment. For example, the neutral buoyance technology suffers from water viscous drag, sealing problems and tremendous burden of safety measures; a parabolic-trajectory flight can simulate zero- or reduced-G for only 10-30 seconds and thus, is too short for training most of the EVA tasks; a counterweight balanced or cable-based suspension system can effectively provide only 1-DOF controlled motion in the vertical direction while the other DOFs are either constrained or with extra forces which do not exist in space; an air-bearing supported system is basically a 2-D simulation; the virtual reality simulation gives only a visual effect without real physical reaction. In short, all these existing reduced-G simulation technologies either cannot generate a full 3-D physical motion (as it would occur in space) or cannot operate in ambient conditions (i.e., a regular lab setting). Hence, there exists motivation to look for innovative reduced-G simulation methods having advantages of low cost, easy implementation and simple operation.

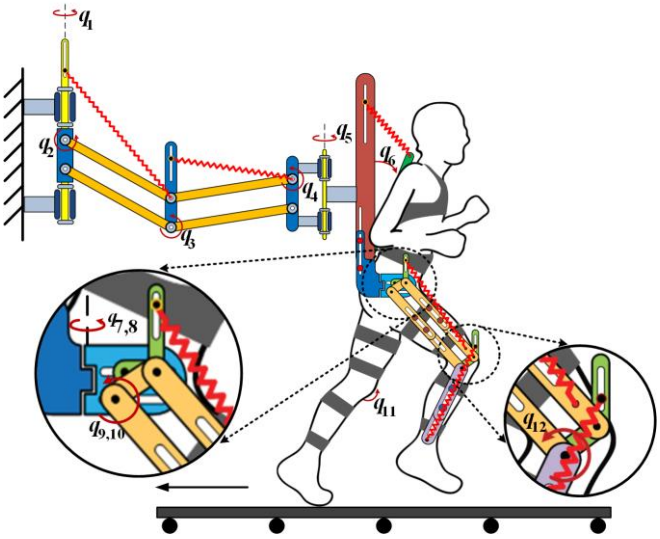

Fig. 1 Concept design of the passive reduced gravity simulator

In this project we are developing a new reduced-G simulation technology for studying human locomotion in a reduced-G (including micro-G) environment. The concept design of such a simulator is shown in Fig. 1. The passive mechanism is designed based on the spring-based passive static balancing technology. Static balancing of a mechanism refers to the status that no joint forces or torques are required to keep the mechanism in static equilibrium for any configuration within its workspace [6, 7]. Therefore, a statically-balanced mechanism can be used to compensate the total or partial gravity force of a person who is attached to the mechanism. Passive static balancing means that no actuators are required to achieve static balancing and thus, the mechanism is a completely passive system. The proposed simulator takes the advantage of the passive static balancing

W. Xiu, K. Ruble and O. Ma are with the Mechanical and Aerospace Engineering Department and the Reduced-Gravity and Biomechanics (RGB) Lab, New Mexico State University, Las Cruces, NM 88003 USA (e-mails: wenwuxiu@nmsu.edu; kruble@nmsu.edu; oma@nmsu.edu).

technology, and allows simulating any desired G level (e.g., 17%G for the lunar gravity or 38%G for the Martian gravity).

Actually, the design of static balancing mechanisms has been an active research topic for several decades (see, for instance, [8] for a recent overview). There are two basic approaches for passive static balancing, namely, using counterweights or using springs [9, 10]. Some gravity-compensated manipulators have been designed using these two approaches [11-13]. Although the counterweight approach is able to achieve static balancing in any direction of the Cartesian space of the mechanism, it introduces additional mass into the system, which results in larger inertia force (or inertial resistance) to the dynamical system. Alternatively, when springs are used for static balancing, the total potential energy (the gravitational energy plus elastic energy) of the mechanism can be kept constant and the weight of the whole mechanism can be balanced using a much smaller added mass than that using the counterweight approach, as pointed out by [14, 15]. The static balancing method has also been introduced to reduce joint torques and improve performance of robots [16, 17]. Recently, a passive gravity-balanced mechanism was proposed to compensate the weight of a patient's arm for rehabilitation [18]. Moreover, passive gravity-balanced leg exoskeletons have also been developed for locomotion training of individuals with leg impairments [19, 20]. The effectiveness of the passive gravity-balancing of such mechanisms on stability issues was studied in [21].

This paper describes the design and an early prototype of a passive reduced-G simulator for aerospace applications. Since the system is based on the static balancing technology, its dynamic performance when applied to a human (which is a complex dynamic system), needs to be investigated.

II. Design and Analysis

A. Kinematics Design

The kinematics of the reduced-G simulator is shown in Fig. 1. It consists of two parallelogram mechanism sections, a torso-support platform, a body harness assembly, and two leg exoskeletons. The system has 12 DOFs represented by joint angles $\theta_1, \theta_2, \cdots, \theta_{12}$, as marked in Fig. 2.

The two parallelogram sections plus the torso-support platform form a 6-joint mechanism which provides a 5-DOF support to the human torso and allows the torso to freely move in the three translational axes and two rotational axes within the workspace of the mechanism. The only constrained rotational DOF is the roll rotation of the torso about a horizontal axis in the sagittal plane. In fact, this motion component is the least significant one in all the 6 motion components during normal human walking. A human leg is known to have 7 DOFs (3 DOFs with the hip joint, 1 DOF with the knee joint, and 3 DOFs with the ankle joint) [22]. The leg exoskeleton, attached to the human thigh (upper leg) and crus (lower leg), has 3 joints, which allows a 2-DOF rotation of the hip joint and 1-DOF rotation of the knee joint. The exoskeleton ends above the ankle joint and thus, it does not constrain any mobility of the ankle joint. This means that the exoskeleton constrains only one of the human leg's seven natural DOFs, which is the hip rotation off the sagittal plane. Based on human gait analysis [22], this rotational motion of a leg is negligible during normal walking. The reasons for having the above-mentioned two constraints in the mechanism design are: 1) the constrained motion components are least significant in a walk gait; 2) it significantly simplified the mechanical design of the system.

B. Gravity Force Compensation

The reduced-G simulator uses seven springs to compensate the weights of the mechanism and the attached human. The arrangement of the springs is shown in Fig. 2. The stiffness values of the springs are denoted by $k_1, k_2, \cdots, k_7$. Among these springs, the first two are attached to the two parallelogram sections, the third one is attached to the torso-support platform, and the fourth and fifth ones are on one leg exoskeleton and the last two are on the other exoskeleton. In the design, we assume that the two legs of a human are identical in both geometric and inertial properties and thus, the springs on both legs are also identical, namely, $k_6 = k_4$ and $k_7 = k_5$.

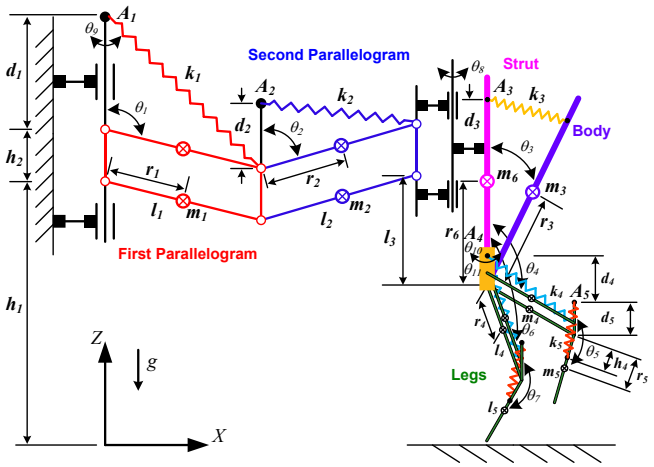

Fig. 2 Kinematic notation of the passive reduced-G simulator

Since we apply the principle of passive static balancing, the total potential energy of the mechanism contributed by both the gravity field and the springs should be constant [14] for all the working configurations of the system in its workspace. This can be mathematically described as

$$V_{Total} = V_{MG} + V_{BG} + V_S = \text{Constant} \qquad (1)$$

where, V_{MG}, V_{BG} and V_S represent the potential energies of the mechanism, human body, and springs, respectively. The condition given by (1) assumes that all the gravity forces are compensated. If just partial gravity effect on the attached human needs to be compensated, (1) should be modified to

$$V_{MG} + \rho V_{BG} + V_S = \text{Constant} \qquad (2)$$

where factor ρ is the ratio of the compensated gravity force over the original gravity force on the human body. Thus, ρ is also the percentage of the human weight to be removed by the mechanism. Note that ρ is a factor of only the potential energy term of the human, because only the human requires a reduced gravity while the gravity of the mechanism has to be fully compensated all the time, so that the attached human does not need to carry any weight of the mechanism.

Based upon the kinematics notation defined in Fig. 2, the total potential energy of the whole system can be expressed in terms of the joint angles as follows:

$$V_{Total} = V_{MG} + \rho V_{BG} + V_S = C_0 + \sum_{i=1}^{7} C_i \cos\theta_i \tag{3}$$

where

$$\begin{aligned}
C_0 &= (2h_1 + h_2)(m_1 + m_2)g + (h_1 - h_3)(M_m + \rho M_B)g \\
&\quad + r_6 m_6 g + 2h_5 m_4 g + \frac{1}{2}k_3(d_3^2 + h_3^2) + k_5(d_5^2 + h_4^2) \\
&\quad + k_4(d_4^2 + l_4^2) + \frac{1}{2}\sum_{i=1}^{2} k_i(d_i^2 + l_i^2) \\
C_1 &= 2m_1 r_1 g + l_1(2m_2 g + M_M g + \rho M_B g - k_1 d_1) \\
C_2 &= 2m_2 r_2 g + l_2(M_M g + \rho M_B g - k_2 d_2) \\
C_3 &= \rho m_3 r_3 g - k_3 d_3 h_3 \\
C_4 &= (2m_4 + \rho m_{ul}) r_4 g + (m_5 + \rho m_{ll}) l_4 g - k_4 d_4 l_4 \\
C_5 &= (m_5 + \rho m_{ll}) r_5 g - k_5 d_5 h_4 \\
C_6 &= C_4, \quad C_7 = C_5 \\
M_m &= 4m_4 + 2m_5 + m_6, \qquad M_B = m_3 + 2m_{ul} + 2m_{ll}
\end{aligned} \tag{4}$$

In (4), m_{ul} and m_{ll} represent the mass values of the upper leg and the lower leg of the human, and the other parameters in the equations have been defined in Fig. 2. It should be pointed out that the elastic potential energy V_S in (3) and (4) is derived based on the assumption that zero-length springs (zero-free length springs) [19] are used in the system.

The only way that guarantees the total energy, as given by (3), to be a constant for all configurations is that all the coefficients in the second term of the right-hand side of (3) become zero. In other words, the conditions for partial gravity balancing (i.e. gravity reduction) are:

$$C_i = 0, \quad i = 1, 2, ..., 7 \tag{5}$$

Based on these conditions, one can calculate a set of spring stiffness values $k_1, k_2, \cdots, k_7$ in terms of the known kinematics and mass parameters of the mechanism and the human. Clearly, using seven springs with the calculated stiffness values will keep the total potential energy of the system as a constant for all the configurations of the mechanism and human because the total potential energy is independent of the configuration variables. In other words, the gravity force on the human body will be compensated to the level defined by parameter ρ.

Note that the set of springs with the calculated stiffness values is only capable of reducing the gravity for a particular person because the spring stiffness values are dependent on the body mass. This means that, when the device is used by a different person, a new set of springs with different stiffnesses has to be used. Obviously, this is inconvenient in practice because every individual has different mass distribution than others and we cannot have so many different sets of springs. A solution to this problem is to use the same set of springs for everyone but leave the springs' attachment points adjustable, namely, to use different sets of the d_i $(i = 1, 2, \cdots, 7)$ values for different people. This is to adjust the attachment points $A_1, A_2, \cdots, A_7$ (see Fig. 2) of the springs based on the mass of the person on the device. The adjustment is also based on (5) assuming fixed spring stiffness values, namely,

$$\begin{aligned}
d_1 &= \frac{2m_1 r_1 + l_1(2m_2 + M_M + \rho M_B)}{l_1 k_1} g \\
d_2 &= \frac{2m_2 r_2 + l_2(M_M + \rho M_B)}{l_2 k_2} g \\
d_3 &= \frac{\rho m_3 r_3}{h_3 k_3} g, \qquad d_5 = d_7 = \frac{(m_5 + \rho m_{ll}) r_5}{h_4 k_5} g \\
d_4 &= d_6 = \frac{(2m_4 + \rho m_{ul}) r_4 + (m_5 + \rho m_{ll}) l_4}{l_4 k_4} g
\end{aligned} \tag{6}$$

The conditions given in (6) are derived based on the assumption that the gravity effect on the human body is partially compensated by the ratio of ρ. If a zero-gravity (0-G) condition is needed, ρ has to be set to 1. For the planetary exploration, one often needs to simulate a reduced-G scenario as opposed to the 0-G condition. This requires a ρ between 0 and 1 depending on the specific application. For example, ρ should be 0.83 for simulating a lunar activity or 0.62 for simulating a Martian activity.

III. Prototype and Experiment

A. Prototype Design

Based on the system design described in Section II, the detailed design and manufacturing work of a prototype of the reduced-G simulator was launched in 2010 in the Reduced-Gravity and Biomechanics Laboratory (RGB Lab) at New Mexico State University. The first prototype was designed and built, as shown in Fig. 4, based on the requirements summarized in Table 1. The system looks larger and stronger than the concept shown in Fig.1 because we had to impose a 2.5 safety factor for human safety. All the load-bearing components of the system were examined using finite element analysis (FEA) software Abaqus under the maximum load conditions. The maximum loads were calculated from dynamic simulations using MSC Adams and LifeMOD. Critical components were over-engineered with strengthened structures or materials. Some materials of noncritical components or areas were reduced for less inertial effect.

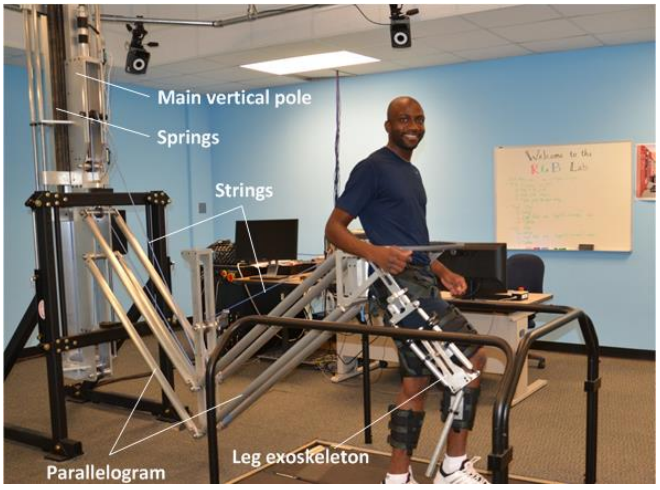

Fig. 4 The complete prototype of the Reduced-G Simulator

Table 1 Major design requirements for the reduced-G simulator

Requirement	Specification
Human weight range	18 ~ 86 kg (40 ~ 190 lb)
Human height range	1.5 ~ 1.85 m (6'1")
Simulated gravity range	from 0G to 1G
Horizontal motion range	1.0 m
Vertical motion range	1.0 m
Maximum walking speed	3.0 m/s
Mobility of the human torso	5 DOFs
Mobility of the human waist	1 DOF
Mobility of each human hip	2 DOFs
Mobility of each human knee	1 DOF
Mobility of other human parts	No limits
Structure safety factor	2.5

A rotational ring was designed and attached around the test subject's waist offering the freedom for the human to twist his/her torso about the waist. The entire 5-DOF mechanism section behind the human torso provides the human with a large enough workspace, such that the person can move within the workspace as freely as possible. A pair of leg exoskeletons was designed to be composed of an upper parallelogram and a lower link, providing gravity offloading to the legs with rotation freedom around the hip and knee joints. The double parallelogram sections, along with the springs on the vertical pole, is used to offload the weight of the whole human body, while the leg exoskeletons and the springs behind the human back are used to compensate the weight of the legs and the feet of the human.

With no "zero length" spring available in reality, it can be challenging to make the linear springs mechanically installed [23]. To solve this problem, we installed the springs with initial tensions in the back of the main vertical pole without destroying the gravity offloading effect (see Fig. 4). This also offered us the advantage of the least inertial effect on the dynamics of the system [24]. Each of the two main springs (i.e., k_1 and k_2) is connected to the outer end of its associated parallelogram section through a multi-pulley and string chain. In order to reduce the amount of the stretch of the springs, each spring is split into four parallel springs. In this way, the height of the main vertical pole and thus, the overall size of the entire system were reduced.

Torso and leg harnesses are necessary system parts to attach the human body to the reduced-G simulator. The selection of the proper harnesses could be challenging, i.e., the harnesses not only need to be strong and rigid enough to support the human weight and secure the body to the equipment but also have to be ergonomically friendly to the human without causing much concentrating force or pressure to the human body. One subjective ergonomic level evaluation method with scores ranging from 1 to 5 was developed for making choices of harnesses out of the commercial available ones. Based on a series of tests of several alternative harnesses with volunteers, we selected our torso harness (originally for movie shooting) and leg harness (originally for medical applications) for the current prototype of the reduced-G simulator.

Although we have built a pair of exoskeletons capable of offloading the weights of the human legs, its ergonomic integration with the torso-support platform of the reduced-G simulator remains a challenging issue. This is because the assembly of the springs (i.e., k_4 and k_6) can easily interfere with the swing arms, which makes the person uncomfortable in walking. We are developing the next generation of the exoskeletons. For the time being, to avoid the discomfort affecting the test subject's walking gait or dynamic behavior, we did not employ the exoskeletons in our presented walking tests. Nevertheless, the actual role of human arms in locomotion gaits and dynamics are still not fully understood [26]. Further, all of the suspension-based reduced-G facilities including NASA's POGS (used for the Apollo program) and ARGOS (used for NASA's current human and robotics space exploration program) do not offload leg weight either [3].

B. Adjustment for Desired Gravity Level

Equation (6) provides the guideline for adjusting the system for a desired weight offloading effect on an attached human. However, we found it challenging to adjust the simulator for a desired G level with different individuals. To solve the problem, an active auto-balancing subsystem was developed, by which different gravity conditions can be reached automatically. In fact, this subsystem allows an actuated adjustment of the spring connection points A_1 and A_2 to fit the attached individual. Details of this adjustment subsystem has been reported in [25]. It should be emphasized that such an adjustment is needed only when switching to a different person or changing the desired G level. Once an adjustment is completed, the auto-balancing subsystem will be turned off and then, the simulator remains fully passive for the operation of the subsequent reduced-G simulation.

C. Setup of the Experimental Test System

In order to investigate the dynamic characteristics of the reduced-G simulator for partial gravity simulation, we have to measure the motion and force data from the attached human body. To this end, a measurement system was installed in the RGB Lab, as shown in Fig.5. The system consists of a Vicon 3D motion capture system with 10 cameras for measuring the human motion data and a Bertec dual-belt instrumented treadmill for measuring the ground reaction force and moment of each foot of the human. Further, the joints of the reduced-G mechanism are also equipped with optical encoders.

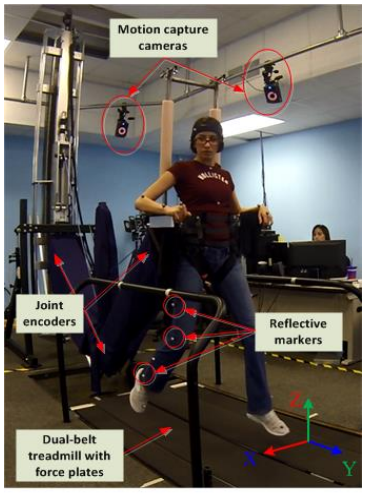

Fig. 5 Measurement system for human subject testing

We have tested the simulator prototype with four student volunteers

recruited from the campus (two males and two females, with an average age 24.8 ± 3.2 years, height 1.73 ± 0.04 m, and mass 59.3 ± 12.7 kg). An IRB (Institutional Review Board) approved informed consent was obtained from each of the test subjects for participation in the study. For quantitative tests and analysis, the tested activities have been limited only to standing, jumping and walking although the system can be used to simulate other human activities.

For each human test, 39 reflective markers (sized 0.5 inch in diameter) were attached to the body segments of the subject to measure the person's kinematic data. The global positions and velocities of these markers were recorded by the Vicon cameras at a sampling rate of 100 Hz. The ground reaction force and the center of pressure (where the ground reaction force exerts) of each foot were measured by the dual-belt instrumented treadmill at a sampling rate of 1000 Hz. The encoder data is also collected from the joints of the simulator mechanism.

In the walking tests, we emphasized to our subjects that they were free to choose their most comfortable walking speed in each gravity case. This was implemented with the following preparation protocol. Prior to actual data collection, a test subject was guided to participate in two exercise sessions to familiarize himself/herself with the simulator's harnesses and treadmill locomotion. First, the subject was asked to walk on the treadmill with the system attachment but without any weight offloading. Our tests showed that a 5-minute exercise is adequate for a participant to feel comfortable with the simulator system for walking on the treadmill. In the second session, the test subject was asked to finish several trials of walking or jumping in different simulated gravity levels. The second session typically took from 10 to 30 minutes for a tested subject. After that, a participant actually found pretty effortless to perform the intended reduced-G test activities on the system.

IV. Experiment Results

The tests of the simulator performed so far were to evaluate the gravity-offload capability, study the performance of the system, and reveal technical issues to be addressed in the future research. We performed nonhuman tests first to make sure that the simulator can compensate the weight of a payload correctly and it is safe enough for human use. After the nonhuman tests were satisfactorily done, we started human subject tests. The main results are described in the next three subsections.

A. Tests of Gravity Compensation Capability

Complete validation of the dynamics of human walking in our simulated reduced-G environment is very difficult simply because no true data (i.e., space-walk data from Moon, Mars or other reduced-G space environments) are available for reference, even for NASA researchers. However, we can still perform some validation exercises through static test cases or nonhuman dynamic test cases.

A first and easiest test is to examine the simulated weight of a person by measuring the ground reaction force while the person is standing still while attached to the simulator. The measured ground reaction force should match the theoretical weight of the person at the simulated G level. Fig. 6 shows the result of such a static test, which is perfectly accurate.

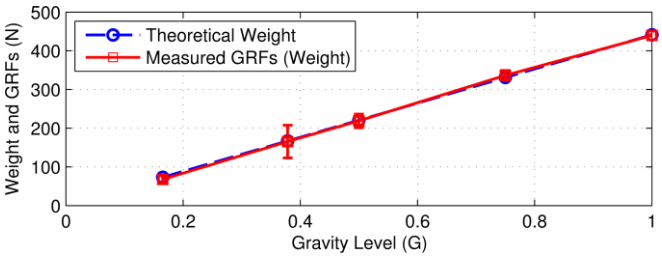

Fig. 6 Measured ground reaction force (GRF) vs simulated G level

The static test method does not apply to the walking case because the weight and ground reaction force are no longer the same in a dynamic case. Since the true dynamics data of human walking in a reduced-G environment is unavailable, we used nonhuman tests. A series of drop tests were done to verify the free-fall time under different gravity levels. In each test an object of known mass was dropped from a known height and allowed it to freely fall to the ground. Its total falling time was recorded and compared to the theoretical free-fall time which can be calculated from $t = \sqrt{2h/g}$, where h and g are the height of the dropping point and desired gravity acceleration, respectively. Fig. 7 illustrates the result of such a set of tests. The test result indicates that the simulator has some error and the error increases with the amount of gravity compensation. Based on our analysis, this error was mainly attributed to the friction in the mechanism as to be discussed in Section IV.D.

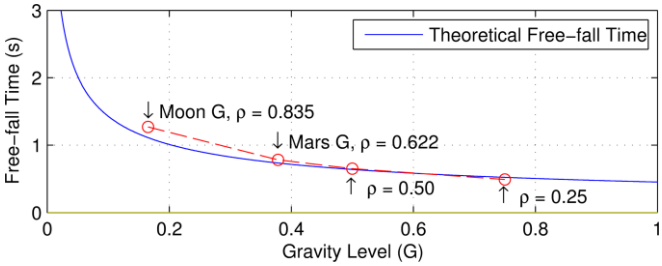

Fig. 7 Theoretical and measured free-fall times for the drop tests

B. Motion Data for Walking in Different Gravity Levels

The accuracy of the simulated gravity effect can also be reflected on the kinematics of human motion in a swing phase [27]. We tested human walking in five different simulated gravity levels specified by: ρ =0, 0.25, 0.5, 2/3, and 5/6. Among these, the ρ=0, ρ=2/3 and ρ=5/6 cases are approximately equal to the Earth gravity (1G), Mars gravity (0.38G) and Moon gravity (0.17G), respectively. Kinematic data representing the body movements of the tested subjects were collected. From these motion data, we can extract various parameters representing the walking gaits.

Plotted in Fig. 8 are typical values of the angle of attack in three different gravity levels. The angle of attack is defined as the supplementary angle of the ankle between a foot and calf of a human, which reflects the flexion extent of the ankle joint during walking. The larger this parameter's range spans, the more dramatic the leg motion is. Obviously, one can see from Fig. 8 that, the more the body weight is removed (e.g., from Earth to Moon), the bigger range of the

test subject to tilt his/her ankle joint. One possible explanation to this phenomenon is that the test subject gains more ability and freedom to move the body with the gravity reduction. Actually, what was observed through the testing is that the test subject chose hopping/skipping instead of walking when the gravity became very low (e.g., in the lunar gravity). In fact, people have noticed such a phenomenon in the NASA videos from the Apollo missions [28].

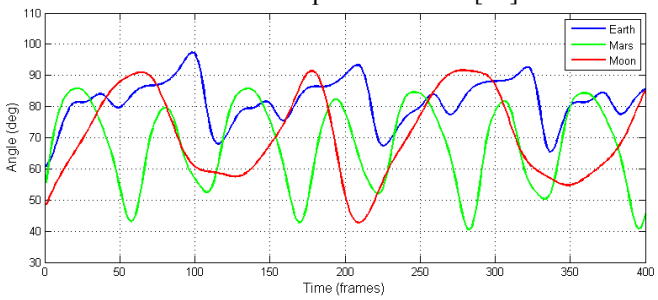

Fig. 8 Measured angle-of-attack data in different simulated G levels

One may notice that the cadence of walking also varies with the gravity level. While the cadence of walking from the Earth gravity to Mars gravity did not change much (both about 0.9 Hz), but that for the lunar gravity dropped to almost an half (about 0.47 Hz). With hopping/skipping as a preferred locomotion gait, the feet of the test subject stayed in air for a longer time (i.e., both feet off the ground for some time, which does not happen in a normal walking gait).

Another interesting kinematic feature to investigate is the stability conditions of walking gaits under different gravity levels. Instead of analyzing the complex dynamics of the human, we observed the distribution of the center of pressure (COP) of the feet as a simple performance index for gait stability. Typical COP distributions with varying gravity levels are shown in Fig. 9. Obviously, the more concentrated a COP distribution is, the more stable the corresponding gait is. As seen from Fig. 9, the boxed boundary roughly represents the area of the COP distribution. As clearly shown, the COP becomes more widely distributed as the gravity is reduced. This might be caused by the less stability of locomotion in a reduced gravity environment. Whether this is an inherent characteristic of the human locomotion in reduced gravity remains to be investigated in the future.

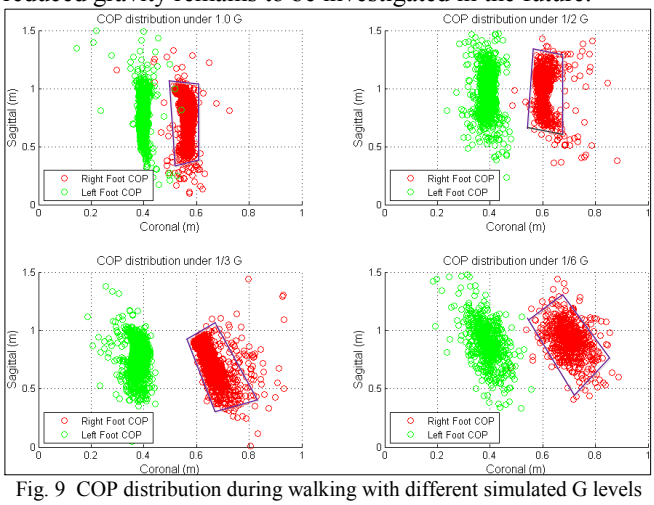

Fig. 9 COP distribution during walking with different simulated G levels

C. Ground Reaction Force in Different Gravity Levels

The magnitude of the ground reaction force of one foot in a typical stance cycle (the period when a foot continuously touches the ground), is plotted in Fig. 10 for comparison. Note that these force profiles are not in the same time scale. As one can see, the force profiles in all the five gravity cases are different from each other. These differences are reflected not only in their shapes but also in their peak values. It is clear that the force gradually decreases with the gravity level except the lunar gravity case (i.e., the 1/6 G case) where the peak force is higher than that in the Mars gravity (i.e., 1/3 G) case. This phenomenon, again, should be caused by the fact that the subject switched to a hopping/skipping gait in the lunar gravity as opposed to just walking as in all the other tested gravity levels. In a skipping mode the ground reaction force is larger because of the shorter and stronger contact between the foot and the ground.

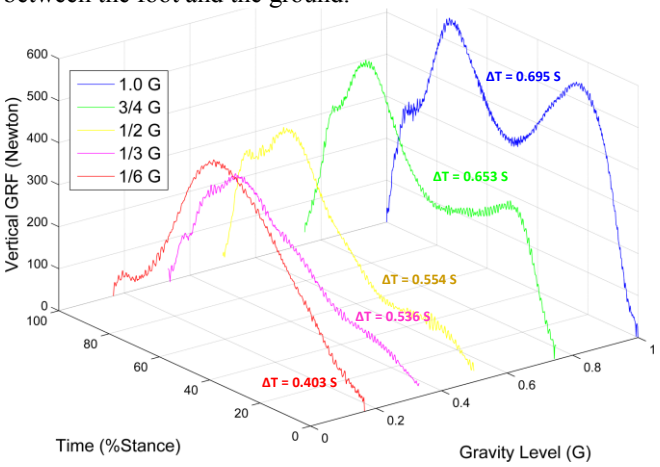

Fig. 10 Ground reaction forces on a foot in different gravity levels

Another obvious phenomenon can be observed from Fig. 10 is that the gait phases change during walking due to the varying gravity. Under the Earth gravity, one can easily see that the stance phase of the gait cycle is composed of two single-support phases and one double-support phase (both feet touching the ground to support the human motion). With the gravity reduced, the double-support phase diminished and finally replaced by a single-support phase in the Moon gravity level. This gait change may be fundamental for further understanding the gait strategy of human locomotion in space environment.

D. Issues Affecting the Fidelity of the Simulator

While still in the concept design stage two years ago, we had anticipated that the joint friction and the mass of the mechanism would be the two main contributing factors limiting the simulation fidelity of the simulator. Our tests done so far indicated that the inertia forces were not a main concern but the joint friction did cause noticeable impedance to the human motion. The observed small inertia effect might be because the acceleration associated with human walking is naturally small and thus, the resulting inertia force is relatively small too. The noticeable friction is mainly from the bearings supporting the pulley-string chains. This is because each pulley applies a very large load on its supporting bearings. The load on a pulley can be as

high as twice the force of its supported spring, generating a large configuration-dependent fictional torque on the supporting bearings [29]. We have had some ideas to reduce the friction effect but the implementation requires significant modification to the current design of the mechanism and thus, it will be studied in future work.

V. Conclusion and Future Work

A reduced-gravity human-rated simulator was designed, built and preliminarily tested. Designed based on the passive static balancing technology, the simulator has demonstrated its capability of passively compensating partial or all the gravity force applied to the attached human body in all the configurations of the simulator. A series of human and nonhuman tests has been conducted for studying the functions and performance of the system. Test data indicated that the simulator is capable of allowing an attached human to biomechanically feel like he/she were in a reduced-gravity environment while walking or jumping with the equipment.

The contribution of this research project is to have demonstrated the feasibility of using the spring-based static balancing technology for compensating the weight of a human body in a multiple-DOF fashion. It opened a completely new application area of the static balancing technology. It provides a new and low-cost microgravity or reduced-gravity simulation technique for training astronauts and studying human factors for future human space exploration missions. It also provides relatively simple and low-cost technology for ordinary people to experience physical activities in a simulated space environment.

The near-time future work includes: a redesign of the leg exoskeleton for better integration with the system, study of friction reduction measures, and improvement of the ergonomic performance of the system.

Acknowledgments

This project was supported by the National Science Foundation through an MRI development grant (#0960156). Technical supports of Dr. R. Paz of the EE Department and Dr. E. Pines of the IE Department at NMSU as well as current and former students Dr. Qi Lu, Dr. Ramon Garcia, Ntengwa Mukosa, Jose Barajas, Jason Wright, Samuel King, Steve Stroup, Brandi Herrera, Gabriela Anguiano-Molina, Rachel Tessier, Ember Krech, Dakota Burrow, etc., who have worked on the project, are highly acknowledged.

References

[1] B. Griffin, "Zero-G simulation verifies EVA servicing of space station modules," *Rep./AIAA*, 1986.

[2] H. A. Fujii, K. Uchiyama, H. Yoneoka, and T. Maruyama, "Ground-based simulation of space manipulators using test bed with suspension system," *Journal of Guidance Control and Dynamics,* vol. 19, pp. 985-991, Sep-Oct, 1996.

[3] T. Cunningham, "System requirements document for the active response gravity offload system (ARGOS)". *NASA Engineering directorate document* AR&SD-08-007. Houston, TX: NASA, 2010.

[4] J. L. Schwartz, M. A. Peck, and C. D. Hall, "Historical review of air-bearing spacecraft simulators," *Journal of Guidance Control and Dynamics,* vol. 26, pp. 513-522, Jul-Aug, 2003.

[5] H. David and G. Charles, "An integrated EVA/RMS virtual reality simulation, including force feedback for astronaut training," in *Flight Simulation Technologies Conference*, ed: American Institute of Aeronautics and Astronautics, 1996.

[6] G. J. Walsh, D. A. Streit, and B. J. Gilmore, "Spatial Spring Equilibrator Theory," *Mechanism and Machine Theory,* vol. 26, pp. 155-170, 1991.

[7] O. Ma, Q. Lu, J. McAvoy, and K. Ruble, "Concept Study of a Passive Reduced-Gravity Simulator for Training Astronauts," in *ASME 2010 Intl. Design Eng. Tech. Conf.*, Montreal, 2010.

[8] Q. Lu, C. Ortega, and O. Ma, "Passive gravity compensation mechanisms: Technologies and applications," *Recent Patents on Engineering,* vol. 5, pp. 32-44, 2011.

[9] I. Ebert-Uphoff, C. m. M. Gosselin, and T. Laliberté, "Static Balancing of Spatial Parallel Platform Mechanisms—Revisited," *Journal of Mechanical Design,* vol. 122, pp. 43-51, 2000.

[10] R. Barents, M. Schenk, W. D. van Dorsser, B. M. Wisse, and J. L. Herder, "Spring-to-Spring Balancing as Energy-Free Adjustment Method in Gravity Equilibrators," *Journal of Mechanical Design,* vol. 133, p. 061010, Jun, 2011.

[11] C. M. Gosselin and J. Wang, "Static balancing of spatial six-degree-of-freedom parallel mechanisms with revolute actuators," *Journal of Robotic Systems,* vol. 17, pp. 159-170, 2000.

[12] L. F. Cardoso, S. Tomázio, and J. L. Herder, "Conceptual Design of a Passive Arm Orthosis," in *ASME International Design Engineering Technical Conferences*, Montreal, 2002.

[13] P. Y. Lin, W. B. Shieh, and D. Z. Chen, "Design of Statically Balanced Planar Articulated Manipulators With Spring Suspension," *Ieee Transactions on Robotics,* vol. 28, pp. 12-21, Feb, 2012.

[14] D. A. Streit and B. J. Gilmore, "Perfect Spring Equilibrators for Rotatable Bodies," *J. of Mechanisms Transmissions and Automation in Design-Transactions of the Asme,* vol. 111, pp. 451-458, Dec, 1989.

[15] C. H. Cho, W. S. Lee, and S. C. Kang, "Design of a Static Balancer with Space Mapping," *International Journal of Precision Engineering and Manufacturing,* vol. 14, pp. 61-68, Jan, 2013.

[16] N. Ulrich and V. Kumar, "Mechanical design methods of improving manipulator performance," in *Advanced Robotics, 'Robots in Unstructured Environments', 91 ICAR., Fifth International Conference on*, 1991, pp. 515-520.

[17] S. Shirata, A. Konno, and M. Uchiyama, "Design and evaluation of a gravity compensation mechanism for a humanoid robot," in *Intelligent Robots and Systems, 2007. IROS 2007. IEEE/RSJ International Conference on*, 2007, pp. 3635-3640.

[18] W. D. Van Dorsser, R. Barents, B. M. Wisse, and J. L. Herder, "Gravity-balanced arm support with energy-free adjustment," *Journal of medical devices,* vol. 1, pp. 151-158, 2007.

[19] A. Fattah and S. K. Agrawal, "On the design of a passive orthosis to gravity balance human legs," *Journal of Mechanical Design,* vol. 127, pp. 802-808, Jul, 2005.

[20] S. K. Banala, S. K. Agrawal, A. Fattah, V. Krishnamoorthy, W. L. Hsu, J. Scholz, *et al.*, "Gravity-balancing leg orthosis and its performance evaluation," *IEEE Trans. on Robotics,* vol. 22, pp. 1228-1239, 2006.

[21] A. Agrawal and S. K. Agrawal, "Effect of gravity balancing on biped stability," in *Robotics and Automation, 2004. Proceedings. ICRA'04. 2004 IEEE International Conference on*, 2004, pp. 4228-4233.

[22] M. W. Whittle, *Gait analysis: an introduction*, 2003.

[23] J. L. Herder, "Energy-free systems: theory, conception, and design of statically balanced spring mechanisms," *Ph.D Thesis*, 2001.

[24] Q. Lu, W. Xiu, and O. Ma, "On the Impedance of Statically-Balanced Mechanisms," in *ASME 2011 International Design Engineering Technical Conferences and Computers and Information in Engineering Conference*, 2011, pp. 543-550.

[25] R. A. Paz, J. C. Barajas, and O. Ma, "Autobalancing control for a reduced gravity simulator," in *Advanced Intelligent Mechatronics (AIM), 2013 IEEE/ASME Intl. Conf. on*, 2013, pp. 405-410.

[26] J. Park, "Synthesis of natural arm swing motion in human bipedal walking," *Journal of biomechanics,* vol. 41, pp. 1417-1426, 2008.

[27] F. Sylos-Labini, Y. P. Ivanenko, G. Cappellini, A. Portone, M. J. MacLellan, and F. Lacquaniti, "Changes of Gait Kinematics in Different Simulators of Reduced Gravity," *Journal of Motor Behavior,* vol. 45, pp. 495-505, Nov 1, 2013.

[28] A. E. Minetti, "The biomechanics of skipping gaits: a third locomotion paradigm?," *Proc Biol Sci,* vol. 265, pp. 1227-35, Jul 7, 1998.

[29] W. Xiu and O. Ma, "Relation between End-Effector Impedance and Joint Friction of Statically-Balanced Mechanisms," *6th Annual Dynamic Systems and Control Conference*, October 21-23, 2013.